



Cite this: *Chem. Commun.*, 2022, 58, 661

Received 21st September 2021,
Accepted 7th December 2021

DOI: 10.1039/d1cc05309d

rsc.li/chemcomm

Evidence of dynamical effects and critical field in a cobalt spin crossover complex†

Thilini K. Ekanayaka,^a Ping Wang,^b Saeed Yazdani,^c Jared Paul Phillips,^c Esha Mishra,^a Ashley S. Dale,^c Alpha T. N'Diaye,^d Christoph Klewe,^d Padraic Shafer,^d John Freeland,^e Robert Streubel,^d James Paris Wampler,^g Vivien Zapf,^g Ruihua Cheng,^{*c} Michael Shatruk^b and Peter A. Dowben^{*,a}

The [Co(SQ)₂(4-CN-py)₂] complex exhibits dynamical effects over a wide range of temperature. The orbital moment, determined by X-ray magnetic circular dichroism (XMCD) with decreasing applied magnetic field, indicates a nonzero critical field for net alignment of magnetic moments, an effect not seen with the spin moment of [Co(SQ)₂(4-CN-py)₂].

Finite temperatures can have a profound influence on the on/off ratio for a molecular memory device, with deleterious consequences.¹ For spintronic device applications, it is important to understand the finite temperature effects on the magnetic moments as the devices will have more practical value if there is reliable operation at room temperature and above.

The majority of molecular magnetic systems are characterized by localized magnetic moments that are randomly oriented at zero applied magnetic field, due to weak exchange coupling between molecules. Under an applied magnetic field, the moments orient with fidelity that depends on the field strength. Although the molecular magnetic moments align along the field, the net magnetization typically decreases with increasing temperature, and the molar magnetic susceptibility scales inversely proportional with the temperature because the thermal excitations of magnons cause spins to misalign with the magnetic field.²

Finite temperature effects obviously occur for molecules where there is a spin state change with temperature. For such spin crossover (SCO) molecules, the magnetic susceptibility deviates from the simple $1/T$ dependence owing to the conversion from the low spin (LS) to the high spin (HS) state, at which point the susceptibility increases with a degree of abruptness, depending on the cooperativity of SCO.^{3–6} At temperatures exceeding the spin state transition temperature, the net measured “collective” magnetic moment in the HS state continues to decrease with temperature.^{3–6} So there are other finite temperature effects beyond the change in spin state, but for SCO molecules and indeed other local moment molecular magnets, this has not been investigated in detail, with just a few exceptions.⁷

Spin crossover (SCO) molecules, including those with valence tautomeric transition, have been studied using X-ray absorption spectroscopy (XAS)^{8,9} at the transition metal L₃-edge to characterize the spin state occupancy^{1,7,10–15} by probing the unoccupied states through the electric dipole-allowed excitation of 2p core electrons into the partially filled spin-split 3d orbitals. If the molecule is photoactive, as is the case with many SCO complexes,^{7,13,15–21} XAS can perturb the spin state by exciting the molecule from the ground LS state *via* intersystem crossing to the metastable HS state, which can be trapped at sufficiently low temperatures. This X-ray fluence induced transition to the high spin state is analogous to such LS-to-HS conversions as light-induced excited spin state trapping (LIESST),^{11,22–26} soft X-ray-induced excited spin state trapping (SOXIESST)^{11,27,28} and hard X-ray-induced excited spin state trapping (HAXIESST).²⁹ If XAS reliably places the molecule in the high spin state, then X-ray magnetic circular dichroism (XMCD) can be used to probe the temperature dependence of relative spin and orbital moment contributions to the local moment. There are, in fact, a few XMCD studies on SCO molecular films. Bernien *et al.*³⁰ performed XMCD to confirm the SOXIESST process for the SCO complex [Fe^{II}(bpz)₂phen] (bpz = dihydrobis(pyrazolyl-1-yl)borate, phen = 1,10-phenanthroline). XMCD has also been employed to establish the influence of the substrate on the spin state occupancy of SCO thin films of [Fe^{II}(phen)₂(NCS)₂].³¹ Apart from a recent study

^a Department of Physics and Astronomy, Jorgensen Hall, University of Nebraska, Lincoln, NE 68588-0299, USA. E-mail: pdowben1@unl.edu

^b Department of Chemistry and Biochemistry, Florida State University, 95 Chieftan Way, Tallahassee, FL 32306, USA

^c Department of Physics, Indiana University-Purdue University Indianapolis, Indianapolis, Indiana 46202, USA

^d Advanced Light Source, Lawrence Berkeley National Laboratory, Berkeley, CA 94720, USA

^e Argonne National Laboratory, Advanced Photon Source, Bldg. 431/E003, 9700 South Cass Ave., Argonne, IL 60439, USA

^f Nebraska Center for Materials and Nanoscience, University of Nebraska-Lincoln, Lincoln, NE 68588, USA

^g National High Magnetic Field Lab, Los Alamos National Laboratory, P.O. Box 1663, Los Alamos, NM 87545, USA

† Electronic supplementary information (ESI) available. See DOI: 10.1039/d1cc05309d

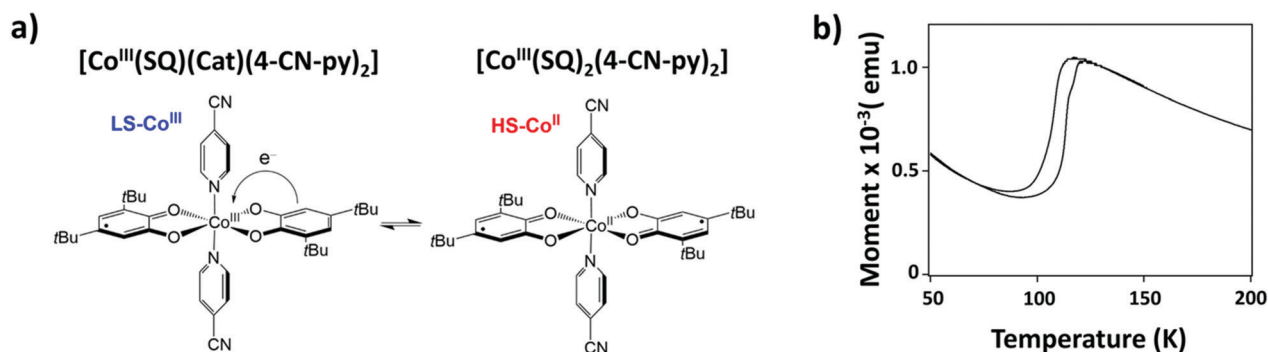


Fig. 1 (a) Schematic diagram of [Co^{III}(SQ)(Cat)(4-CN-py)₂] in LS state and [Co(SQ)₂(4-CN-py)₂] in HS state. The arrow indicates the direction of temperature- or radiation-induced ligand-to-metal electron transfer that converts the LS-Co(III) center into the HS-Co(II) center. (b) Magnetic susceptibility of [Co(SQ)(Cat)(4-CN-py)₂]/[Co(SQ)₂(4-CN-py)₂] powder prior to thin film fabrication.

on the SCO complex [Fe(bpz)₂(bipy)] (bipy = 2,2'-bipyridine),⁷ there have been no studies reported to observe the relative spin and orbital moment contributions to the local magnetic moment.

In this study, we report the temperature- and field-dependent XMCD of a cobalt complex that exhibits a valence tautomeric transition^{23,24,32,33} from the LS [Co^{III}(SQ)(Cat)(4-CN-py)₂] to the HS [Co^{II}(SQ)₂(4-CN-py)₂], where Cat = 3,5-di-*tert*-butylcatecholate, SQ = 3,5-di-*tert*-butylsemiquinonate, and 4-CN-py = 4-cyanopyridine. With the spin transition at the metal center, an electron from the diamagnetic catecholate (Cat²⁺) ligand is transferred to the LS-Co(III) center which yields a HS-Co(II) ion and a radical semiquinonate (SQ⁻) ligand.^{23,24} This valence tautomeric transition is schematically shown in Fig. 1a. The LIESST state induced by photo-conversion from the LS [Co^{III}(SQ)(Cat)(4-X-py)₂] to HS [Co^{II}(SQ)₂(4-X-py)₂] is long lived below 50 K and, while observed up to 90 K,^{23,24} is increasingly short lived for X = CN,^{23,24} Br,²⁴ and NO₂.²⁴

The complex [Co^{II}(SQ)₂(4-X-py)₂] was synthesized as described previously^{23,24,29,33} (see the ESI† for further details). The 100 nm-thick [Co^{II}(SQ)₂(4-X-py)₂] thin film was deposited onto a highly-oriented pyrolytic graphite (HOPG) substrate as described in the ESI,† where we also provide considerable evidence that [Co^{II}(SQ)₂(4-X-py)₂] preserves its molecular structure when deposited as a thin film. HOPG was chosen because this is one of the few substrates that have little influence on the spin state of a SCO molecule.^{25,26,30}

Field dependent XMCD spectroscopy was performed at the Advanced Photon Source beamline 4-ID-C at Argonne National Laboratory. The XMCD spectra near the Co L_{2,3}-edge were obtained at 200 K and magnetic bias fields (0.5 to 2 T μ₀⁻¹). The temperature dependent X-ray absorption and XMCD spectroscopy were carried out at the Advanced Light Source bending magnet beamline 6.3.1 and undulator beamline 4.0.2 at Lawrence Berkeley National Laboratory using a magnetic field of 3.6 T μ₀⁻¹ for the XMCD. Both the XAS and XMCD spectra were acquired in the total electron yield mode, and for the XMCD results presented here, the applied magnetic field was normal to the plane of the thin film. Since this magnetic field strength is insufficient to align and saturate the magnetic moments, the measured values for the spin and

orbital moments will be a small fraction of the actual Co(II) moments. We also note that the various beamlines employed for this study differ in the ellipticity of the light, resulting in variations in the XMCD spectra, particularly variations in the spin to orbital moment ratios plotted in Fig. 3 and 4.

Temperature-dependent X-ray photoemission spectroscopy (XPS) measurements were taken as a function of temperature at photon energy of 1486.6 eV (Al Kα X-ray source) with a SPECS PHOIBOS 150 hemispherical energy analyzer with 20 eV pass energy.²²

The temperature dependent magnetic susceptibility data of [Co(SQ)₂(4-CN-py)₂] reveal a spin state transition temperature of about 110 K and a hysteresis of 5 K (Fig. 1b), in agreement with previous observations.²³ In the LS state, the complex exists in the S = 1/2 ground state due to the unpaired electron of the SQ radical. In the HS state, the magnetic susceptibility is due to contributions from the S = 3/2 HS Co(II) ion and two S = 1/2 SQ radicals. In contrast to the magnetic data, the XAS spectra (Fig. 2a) show little evidence of a spin state transition. Some small changes are observed between 50 to 250 K, but these changes are almost negligible (see the ESI† for further details). The multiplet fitting of the XPS spectra at 220 K to 300 K are also shown in Fig. 2b. The peak shape of the XPS spectrum

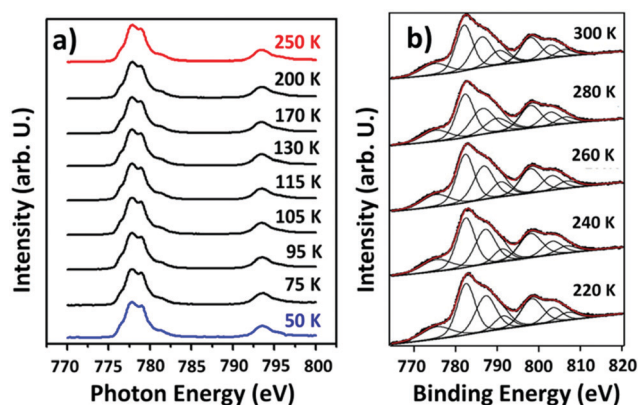


Fig. 2 Temperature dependent XAS (a) and XPS (b) spectra, taken at Co 2p core level, of a [Co(SQ)₂(4-CN-py)₂] thin film.

remains unaffected by temperature, indicating the absence of a redistribution of multiplet intensities known to accompany SCO in transition metal complexes.^{18,22,34,35} These observations indicate that the system, exposed to soft X-ray fluence, is mostly in the HS state even at low temperature, which is consistent with the small change in bond lengths reported elsewhere.³³

Field and temperature dependent XMCD measurements near the Co 2p_{3/2} (L₃) and 2p_{1/2} (L₂) edges were performed (Fig. 3 and 4) to ascertain the behavior of the spin and orbital magnetic moments. The XMCD intensity increases with the magnetic field (Fig. 3b). The orbital and spin moments are calculated from the integrals of both XAS and XMCD spectra (dashed lines in Fig. 3a and b) defined as,³⁶

$$r = \int_{L_3+L_2} (\mu_+ + \mu_-) d\omega, q = \int_{L_3+L_2} (\mu_+ - \mu_-) d\omega \text{ and } p = \int_{L_3} (\mu_+ - \mu_-) d\omega,$$

where μ_+ and μ_- are the XAS intensities taken with left and right circular polarization or opposing applied magnetic fields. The orbital and spin moments are shown in Fig. 3c with respect to the applied magnetic field strength.

The linear increase with magnetic field indicates that both spin and orbital moments are not saturated at an applied field of 2 T μ_0^{-1} . Extrapolation of the spin moment to zero at zero applied magnetic field corroborates a negligible net remanence magnetization indicative of paramagnetic behavior. While both the spin and orbital moment decrease with decreasing magnetic field, the orbital moment has a critical field barrier of 3.4 kOe. This means that a critical field is required for the orbital moments to become evident. As shown in the ESI† materials, choosing different subsets of the available data could reduce the critical field to 1.6 kOe, but not to zero.

Such critical fields stem from barriers caused by the ligand field in the [Co(SQ)₂(4-CN-py)₂] complex, including anisotropy barriers (see the ESI† for a more detailed discussion). The ratio of the spin to orbital moment, estimated from the XMCD

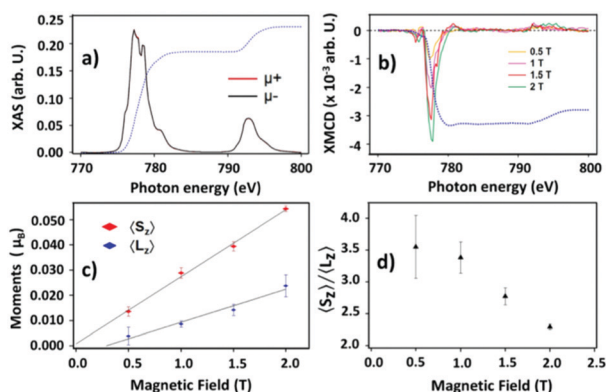


Fig. 3 Field dependent XMCD on [Co(SQ)₂(4-CN-py)₂] thin films in the HS state on HOPG at 200 K. (a) XAS spectra and (b) field dependent XMCD signal at Co L-edge. (c) Spin and orbital moments with respect to applied magnetic field. (d) Spin to orbital moment ratio with respect to magnetic field.

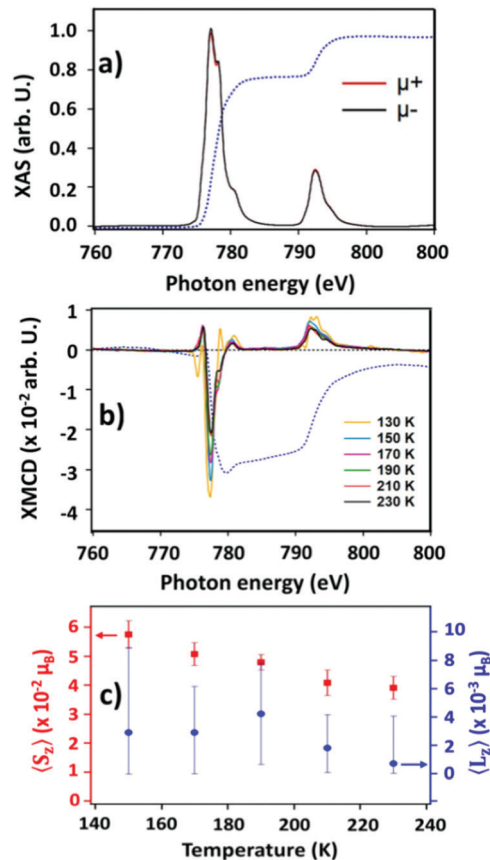


Fig. 4 Temperature dependent XMCD for [Co(SQ)₂(4-CN-py)₂] thin films on HOPG. (a) X-ray absorption spectra and (b) temperature dependent XMCD signal at Co L-edge. (c) Spin and orbital moments with respect to temperature.

spectra according to $\langle S_z \rangle / \langle L_z \rangle = (9p-6q)/2q$,³⁶ is shown in Fig. 3d. Here, p and q are obtained from the integrated XMCD signals at the L₃ and L₂ edges, respectively, as shown in Fig. 3b. The $\langle S_z \rangle / \langle L_z \rangle$ ratio decreases with increasing magnetic field from 3.6 at 0.5 T μ_0^{-1} to 2.2 at 2 T μ_0^{-1} , which agrees well with the expected spin to orbital moment ratio for the HS-Co(II) ion (3.44 to 2.3).³⁷

The temperature dependent XMCD of a 100 nm-thick film of [Co(SQ)(Cat)(4-CN-py)₂] on a HOPG substrate is shown in Fig. 4. The data were recorded in the presence of a magnetic field 3.6 T μ_0^{-1} to increase the signal-to-noise ratio. As seen in Fig. 4b, the XMCD signal decreases with increasing temperature. The spin and orbital moments are calculated using the sum rules³⁵ and integrals of XAS and XMCD spectra (Fig. 4a and b) and shown in Fig. 4c. When increasing the temperature from 150 K to 250 K, the spin moment (Fig. 4c) shows a significant decrease consistent with the decline in overall moment above 140 K (Fig. 1b). This change can be attributed to thermal magnon excitations which cause a spin moment misalignment even with an applied magnetic field. The resulting projection of spins in the minority spin channel decreases the net spin moment, consistent with the decreasing magnetization with temperature seen in Fig. 1b. While the present XMCD results

indicate that the spin moment is sensitive to temperature, for another SCO system, $[\text{Fe}\{\text{H}_2\text{B}(\text{pz})_2\}_2(\text{bipy})]$, the orbital moment, not the spin moment, was found to be sensitive to temperature.⁷

It is evident that, even in the HS state, $[\text{Co}(\text{SQ})_2(4\text{-CN-py})_2]$ exhibits a barrier to orbital moment alignment while the spin moment is clearly temperature dependent. While $[\text{Co}(\text{SQ})_2(4\text{-CN-py})_2]$ is a photoactive material, easily excited from the LS-Co^{III} to the HS-Co^{II} state, it should be noted that finite temperature effects are likely to affect all local moment molecular systems.

This research was supported by the National Science Foundation through NSF-DMR 2003057 [T. Ekanayaka, Ashley S. Dale, Esha Mishra, Ruihua Cheng, P. A. Dowben] and a Nebraska EPSCoR FIRST Award #OIA-1557417 [R. Streubel]. Use of the Advanced Light Source, Lawrence Berkeley National Laboratory, was supported by the U.S. Department of Energy (DOE) under contract no. DE-AC02-05CH11231, while use of the Advanced Photon Source was supported by DOE's Office of Science under contract DE-AC02-06CH11357. The synthesis and magnetic characterization of the complex was carried out by the Shatruck and Zapf groups within the Center for Molecular Magnetic Quantum Materials, an Energy Frontier Research Center funded by the U.S. Department of Energy, Office of Science, Basic Energy Sciences under Award no. DE-SC0019330.

Conflicts of interest

There are no conflicts to declare.

References

- G. Hao, R. Cheng and P. A. Dowben, *J. Phys.: Condens. Matter*, 2020, **32**, 234002.
- J. S. Miller and M. Drillon, *Magnetism: molecules to materials*, Wiley-VCH, Weinheim, New York, 2001.
- A. Bousseksou, G. Molnár, L. Salmon and W. Nicolazzi, *Chem. Soc. Rev.*, 2011, **40**, 3313.
- P. Gülich and H. A. Goodwin, *Spin crossover in transition metal compounds I-III*, Springer, Berlin, New York, 2004.
- P. Gülich, A. Hauser and H. Spiering, *Angew. Chem., Int. Ed. Engl.*, 1994, **33**, 2024–2054.
- M. A. Halcrow, *Spin-crossover materials: properties and applications*, Wiley, Chichester, West Sussex, United Kingdom, 2013.
- G. Hao, A. T. N'Diaye, T. K. Ekanayaka, A. S. Dale, X. Jiang, E. Mishra, C. Mellinger, S. Yazdani, J. W. Freeland, J. Zhang, R. Cheng, X. Xu and P. A. Dowben, *Magnetochemistry*, 2021, **7**, 135.
- G. Poneti, M. Mannini, L. Sorace, P. Sainctavit, M.-A. Arrio, E. Otero, J. Criginski Cezar and A. Dei, *Angew. Chem., Int. Ed.*, 2010, **49**, 1954–1957.
- H. W. Liang, T. Kroll, D. Nordlund, T.-C. Weng, D. Sokaras, C. G. Pierpont and K. J. Gaffney, *Inorg. Chem.*, 2017, **56**, 737–747.
- X. Zhang, P. S. Costa, J. Hooper, D. P. Miller, A. T. N'Diaye, S. Beniwal, X. Jiang, Y. Yin, P. Rosa, L. Routaboul, M. Gonidec, L. Poggini, P. Braunstein, B. Doudin, X. Xu, A. Enders, E. Zurek and P. A. Dowben, *Adv. Mater.*, 2017, **29**, 1702257.
- B. Warner, J. C. Oberg, T. G. Gill, F. El Hallak, C. F. Hirjibehedin, M. Serrì, S. Heutz, M.-A. Arrio, P. Sainctavit, M. Mannini, G. Poneti, R. Sessoli and P. Rosa, *J. Phys. Chem. Lett.*, 2013, **4**, 1546–1552.
- X. Zhang, A. T. N'Diaye, X. Jiang, X. Zhang, Y. Yin, X. Chen, X. Hong, X. Xu and P. A. Dowben, *Chem. Commun.*, 2018, **54**, 944–947.
- X. Zhang, S. Mu, G. Chastanet, N. Daro, T. Palamarciuc, P. Rosa, J.-F. Létard, J. Liu, G. E. Sterbinsky, D. A. Arena, C. Etrillard, B. Kundys, B. Doudin and P. A. Dowben, *J. Phys. Chem. C*, 2015, **119**, 16293–16302.
- G. Hao, A. Mosey, X. Jiang, A. J. Yost, K. R. Sapkota, G. T. Wang, X. Zhang, J. Zhang, A. T. N'Diaye, R. Cheng, X. Xu and P. A. Dowben, *Appl. Phys. Lett.*, 2019, **114**, 032901.
- B. Rösner, M. Milek, A. Witt, B. Gobaut, P. Torelli, R. H. Fink and M. M. Khusniyarov, *Angew. Chem.*, 2015, **127**, 13168–13172.
- C. Etrillard, V. Faramarzi, J.-F. Dayen, J.-F. Létard and B. Doudin, *Chem. Commun.*, 2011, **47**, 9663.
- F. Guillaume, Y. A. Tobon, S. Bonhommeau, J.-F. Létard, L. Moulet and E. Freysz, *Chem. Phys. Lett.*, 2014, **604**, 105–109.
- L. Poggini, M. Gonidec, J. H. González-Estefan, G. Pecastaings, B. Gobaut and P. Rosa, *Adv. Electron. Mater.*, 2018, **4**, 1800204.
- Y. Hasegawa, S. Kume and H. Nishihara, *Dalton Trans.*, 2009, 280–284.
- K. Takahashi, Y. Hasegawa, R. Sakamoto, M. Nishikawa, S. Kume, E. Nishibori and H. Nishihara, *Inorg. Chem.*, 2012, **51**, 5188–5198.
- M. Milek, F. W. Heinemann and M. M. Khusniyarov, *Inorg. Chem.*, 2013, **52**, 11585–11592.
- T. K. Ekanayaka, H. Kurz, A. S. Dale, G. Hao, A. Mosey, E. Mishra, A. T. N'Diaye, R. Cheng, B. Weber and P. A. Dowben, *Mater. Adv.*, 2021, **2**, 760–768.
- R. D. Schmidt, D. A. Shultz and J. D. Martin, *Inorg. Chem.*, 2010, **49**, 3162–3168.
- R. D. Schmidt, D. A. Shultz, J. D. Martin and P. D. Boyle, *J. Am. Chem. Soc.*, 2010, **132**, 6261–6273.
- L. Kippen, M. Bernien, F. Nickel, H. Naggert, A. J. Britton, L. M. Arruda, E. Schierle, E. Weschke, F. Tuczek and W. Kuch, *J. Phys.: Condens. Matter*, 2017, **29**, 394003.
- L. Kippen, M. Bernien, S. Ossinger, F. Nickel, A. J. Britton, L. M. Arruda, H. Naggert, C. Luo, C. Lotze, H. Ryll, F. Radu, E. Schierle, E. Weschke, F. Tuczek and W. Kuch, *Nat. Commun.*, 2018, **9**, 2984.
- A. Mohamed, M. Lee, K. Kitase, T. Kitazawa, J.-Y. Kim and D.-Y. Cho, *Crystals*, 2018, **8**, 433.
- D. Collison, C. D. Garner, C. M. McGrath, J. F. W. Mosselmanns, M. D. Roper, J. M. W. Seddon, E. Sinn and N. A. Young, *J. Chem. Soc., Dalton Trans.*, 1997, 4371–4376.
- T. M. Francisco, W. J. Gee, H. J. Shepherd, M. R. Warren, D. A. Shultz, P. R. Raithby and C. B. Pinheiro, *J. Phys. Chem. Lett.*, 2017, **8**, 4774–4778.
- M. Bernien, *et al.*, *ACS Nano*, 2015, **9**, 8960–8966.
- T. Miyamachi, M. Gruber, V. Davesne, M. Bowen, S. Boukari, L. Joly, F. Scheurer, G. Rogez, T. K. Yamada, P. Ohresser, E. Beaurepaire and W. Wulfhekel, *Nat. Commun.*, 2012, **3**, 938.
- E. Evangelio and D. Ruiz-Molina, *C. R. Chim.*, 2008, **11**, 1137–1154.
- M. A. Ribeiro, D. E. Stasiw, P. Pattison, P. R. Raithby, D. A. Shultz and C. B. Pinheiro, *Cryst. Growth Des.*, 2016, **16**, 2385–2393.
- L. Poggini, M. Milek, G. Londi, A. Naim, G. Poneti, L. Squillantini, A. Magnani, F. Totti, P. Rosa, M. M. Khusniyarov and M. Mannini, *Mater. Horiz.*, 2018, **5**, 506–513.
- J.-Y. Son, K. Takubo, D. Asakura, J. W. Quilty, T. Mizokawa, A. Nakamoto and N. Kojima, *J. Phys. Soc. Jpn.*, 2007, **76**, 084703.
- C. T. Chen, Y. U. Idzerda, H.-J. Lin, N. V. Smith, G. Meigs, E. Chaban, G. H. Ho, E. Pellegrin and F. Sette, *Phys. Rev. Lett.*, 1995, **75**, 152–155.
- B. Weber, *Koordinationschemie: Grundlagen und aktuelle Trends*, Springer Spektrum, Berlin Heidelberg, 2014.